Calhoun
Institutional Archive of the Naval Postgraduate School

Calhoun: The NPS Institutional Archive

DSpace Repository

Theses and Dissertations | 1. Thesis and Dissertation Collection, all items

1982

Tactical application of an atmospheric mixed-layer model.

Graves, Ronald M.

Monterey, California. Naval Postgraduate School

http://hdl.handle.net/10945/20369

This publication is a work of the U.S. Government as defined in Title 17, United States Code, Section 101. Copyright protection is not available for this work in the United States.

Downloaded from NPS Archive: Calhoun

http://www.nps.edu/library

Calhoun is the Naval Postgraduate School's public access digital repository for research materials and institutional publications created by the NPS community. Calhoun is named for Professor of Mathematics Guy K. Calhoun, NPS's first appointed -- and published -- scholarly author.

Dudley Knox Library / Naval Postgraduate School
411 Dyer Road / 1 University Circle
Monterey, California USA 93943

GRADUATE SCHOOL

NAVAL POSTGRADUATE SCHOOL
Monterey, California

THESIS

TACTICAL APPLICATION

OF AN ATMOSPHERIC MIXED-LAYER MODEL

by

Ronald Morton Graves

December 1982

Thesis Advisor: K. L. Davidson

Approved for public release; distribution unlimited

T207937

LIBRARY, NAVAL POSTGRADUATE SCHOOL
MONTEREY, CA 93940

SECURITY CLASSIFICATION OF THIS PAGE (When Data Entered)

REPORT DOCUMENTATION PAGE		READ INSTRUCTIONS BEFORE COMPLETING FORM
1. REPORT NUMBER	2. GOVT ACCESSION NO.	3. RECIPIENT'S CATALOG NUMBER
4. TITLE (and Subtitle) Tactical Application of an Atmospheric Mixed-Layer Model		5. TYPE OF REPORT & PERIOD COVERED Master's Thesis December 1982 6. PERFORMING ORG. REPORT NUMBER
7. AUTHOR(s) Ronald Morton Graves		8. CONTRACT OR GRANT NUMBER(s)
9. PERFORMING ORGANIZATION NAME AND ADDRESS Naval Postgraduate School Monterey, California 93940		10. PROGRAM ELEMENT, PROJECT, TASK AREA & WORK UNIT NUMBERS
11. CONTROLLING OFFICE NAME AND ADDRESS Naval Postgraduate School Monterey, California 93940		12. REPORT DATE December 1982 13. NUMBER OF PAGES 58
14. MONITORING AGENCY NAME & ADDRESS(if different from Controlling Office)		15. SECURITY CLASS. (of this report) Unclassified 15a. DECLASSIFICATION/DOWNGRADING SCHEDULE

16. DISTRIBUTION STATEMENT (of this Report)

Approved for public release; distribution unlimited.

17. DISTRIBUTION STATEMENT (of the abstract entered in Block 20, if different from Report)

18. SUPPLEMENTARY NOTES

19. KEY WORDS (Continue on reverse side if necessary and identify by block number)

Ducting	Electromagnetic propagation	Subsidence
Refraction	Single-station assessment	Duct prediction
Environment	Single-station forecasting	Mixed layer
Environmental effects	Marine atmospheric mixed-layer	

20. ABSTRACT (Continue on reverse side if necessary and identify by block number)

Modern Naval weapon and sensor systems are strongly influenced by the marine environment. Foremost among the atmospheric effects is ducting of electromagnetic energy by refractive layers in the atmosphere. To assess the effect of ducting on electromagnetic emissions, the Navy developed the Integrated Refractive Effects Prediction System (IREPS). Research at Naval Postgraduate School (NPS) has led to development of a state-of-the-art model

(CONTINUED)

20. ABSTRACT (continuation).

which can be used to predict changes to the refractive profile of the lower atmosphere. The model uses radiosonde data and surface meteorological observations to predict changes in refractive conditions and low level cloud/fog formation over 18 to 30 hour periods. The model shows some skill in forecasting duct regions when subsidence rates can be specified to within +/-.0015 m/s. This tesis shows the applicability of the NPS marine atmospheric mixed layer model to fleet tactics. Atmospheric refractive effects on specific emitters can be predicted when model predictions are used in conjunction with IREPS.

Approved for public release; distribution unlimited

Tactical Application of an Atmospheric Mixed-Layer Model

by

Ronald M. Graves
Lieutenant, United States Navy
B.S., University of Washington, 1977

Submitted in partial fulfillment of the
requirements for the degree of

MASTER OF SCIENCE IN METEOROLOGY AND OCEANOGRAPHY

from the

NAVAL POSTGRADUATE SCHOOL
December 1982

C.1

ABSTRACT

Modern Naval weapon and sensor systems are strongly influenced by the marine environment. Foremost among the atmospheric effects is ducting of electromagnetic energy by refractive layers in the atmosphere. To assess the effect of ducting on electromagnetic emissions, the Navy developed the Integrated Refractive Effects Prediction System (IREPS). Research at Naval Postgraduate School (NPS) has led to development of a state-of-the-art model which can be used to predict changes to the refractive profile of the lower atmosphere. The model uses radiosonde data and surface meteorological observations to predict changes in refractive conditions and low level cloud/fog formation over 18 to 30 hour periods. The model shows some skill in forecasting duct regions when subsidence rates can be specified to within +/-.0015 m/s. This thesis shows the applicability of the NPS marine atmospheric mixed layer model to fleet tactics. Atmospheric refractive effects on specific emitters can be predicted when model predictions are used in conjunction with IREPS.

TABLE OF CONTENTS

I. INTRODUCTION 9

II. THE MODEL DESCRIPTION 14

A. MODEL OVERVIEW 14

B. BASIC MODEL EQUATIONS 17

C. SATELLITE DATA INPUT TO MODEL 21

III. ARABIAN SEA CLIMATOLOGY AND SYNOPTIC DESCRIPTION . 22

A. CLIMATOLOGY 22

B. SYNOPTIC CONDITIONS 23

IV. THE MODEL PERFORMANCE 28

A. DUCT PREDICTION 28

B. CLOUD PREDICTION 33

C. EXAMINATION OF MODEL SENSITIVITY 38

V. TACTICAL APPLICATIONS 44

VI. CONCLUSIONS AND RECOMMENDATIONS 52

APPENDIX A. RADIOSONDE TIMES AND LOCATIONS 55

LIST OF REFERENCES 56

INITIAL DISTRIBUTION LIST 57

LIST OF FIGURES

Figure 1. Regional Chart Showing Sounding Data Locations. 13

Figure 2. NPS Mixed Layer Model Functional Block Diagram. 16

Figure 3. Vertical Structure of θ, q and Corresponding M Profile for a Typical Inversion (Model Simplification is Dashed). 20

Figure 4. Frequency of Elevated Duct Occurrence During Spring, after Lammers et al (1980). 23

Figure 5. Hadley Cell and Subtropical Jet Position Showing Area of Maximum Downward Motion, after Palmen and Newton (1969). 27

Figure 6. Model Predicted Ducts (dashed) vs. Observed Ducts (solid) for the Period 6-8 February 1980. 30

Figure 7. Model Prediction Showing LCL Dropping Beneath the Inversion at 2100 11 Feb. 34

Figure 8. NOAA 6 Satellite IR Imagery from 0800 13 February Showing the Presence of Stratus Clouds. 35

Figure 9. Model Prediction 0300 14 to 0900 15 February. 36

Figure 10. NOAA 6 Satellite IR Imagery from 15 February. 36

Figure 11. Model Prediction 0700 21 to 1300 22 February. 37

Figure 12. NOAA 6 Satellite IR Imagery 0800 21 February. 37

Figure 13. Initial Surface Search Radar Coverage 0420 7 Feb 80. 47

Figure 14. Surface Search Radar Coverage 0333 8 Feb 80 Based on Actual Sounding (l) and Model Prediction (r). 47

Figure 15. Surface Search Radar Coverage 0240 9 Feb 80 Based on Actual Sounding (l) and Model Prediction (r). 48

LIST OF TABLES

TABLE I. Data Area Cloud Coverage 8-21 February 1980. 24

TABLE II. Calculated Subsidence Rates 26

TABLE III. Comparison of Observed Duct Heights With Model Predicted Heights Using Hindcast Subsidence Values. 29

TABLE IV. Comparison of Observed Ducts with Model Predicted Ducts Assuming Persistent Subsidence. 32

TABLE V. Error Analysis of Model Prediction vs. Persistence. 33

TABLE VI. Sensitivity of Model Duct Predictions to SST and Wind Variations. 39

TABLE VII. Sensitivity of Model Duct Predictions to Subsidence. 43

TABLE VIII. Radiosonde Data Set. 55

TABLE IX. Radiosondes Used in Model Performance Runs. 55

ACKNOWLEDGEMENT

The insights provided by Lieutenant Commander Corbin of the Naval Oceanography Command Detachment were very helpful in verifying, through his first-hand experience in the Indian Ocean, the great extent of EM ducting in the region and its operational impact on naval forces. Captain Wayne P. Hughes of NPS provided many thought-provoking comments on naval tactics and generously spent time reviewing the tactical applications chapter of this thesis. Thanks are also due Professor Wash for his help in interpreting the satellite imagery and to Professor Haney, who willingly spent considerable time and effort reviewing my work and offering constructive criticism. Mike McDermet, responsible for the high quality illustrations, saved me a great deal of time and effort through his expertise in drafting. Finally, thanks to Professor Ken Davidson, who initially sparked my interest in EM ducting, and who provided the steady encouragement and continual review of my work which made the effort worthwhile.

I. INTRODUCTION

Over the centuries military leaders have learned to appreciate and take advantage of the effects of the environment, and when they failed to do so, have met with disaster. As it approached the islands of Japan in the thirteenth century, Ghengis Khan's Mongol invasion fleet was destroyed by a typhoon. From August to October 1588 the Spanish Armada was beset by storm after storm which resulted in the sinking of many ships and failure of Spain's attempted invasion of Britain. On D-Day, June 6, 1944, the allied invasion force took advantage of predicted good weather between storms and made the amphibious assault across the beaches of Normandy. In December of the same year Admiral Halsey's Third Fleet was caught preparing to refuel by an undetected typhoon, causing 28 ships to be crippled, 156 airplanes to be lost, and the destroyers SPENCE, MONAGHAN, and HULL to be sunk (Nash 1976).

Modern naval warfare technology is providing increasingly capable and complex, but environmentally dependent weapons/sensor systems. Not only the severe sea and weather conditions must be predicted to retain advantage over adversaries, but also environmental factors which enhance or

degrade a wide range of weapon and sensor systems which utilize electromagnetic (EM) propagation. Electromagnetic frequencies above the HF (3-30Mhz) band can be greatly affected by atmospheric refraction.

A condition known as ducting occurs when a refractive layers cause EM energy to bend toward the earth at a rate greater than or equal to the earth's curvature. Ducting occurs with certain critical vertical gradients of temperature and humidity, and can cause both increased radar and radio ranges, and holes (gaps) in normal coverage.

Tactical advantages exist by knowing duct locations. These advantages include being able to make realistic estimates of ESM detection and counter detection ranges. This would enable commanders to make decisions concerning emission control (EMCON), the positioning of both air and surface surveillance assets, the altitude and flight profiles for strike aircraft to minimize detection, the placement of electronic jammers for maximum effect, and numerous other tactical considerations.

Ducting commonly occurs with inversions which act as trapping layers, refracting or bending EM energy toward the earth. Inversions are stable layers between warm, dry air

aloft and cooler, more moist air below and typically exist in marine surface high pressure regions. Extensive areas of low level stratus clouds often delineate areas of duct occurrence.

Ducting is expected to be minimal near fronts and areas of convective cloudiness. Fronts, with their associated upward motion, often dissipate the inversions as the whole air column becomes mixed. Areas of convective activity, detectible by the presence of cumulus clouds, are also normally inversion free. Thus satellite infrared (IR) and visible photography should provide means to estimate ducting regimes.

The Navy employs a microcomputer based system, IREPS (Integrated Refractive Effects Prediction System) (Hitney, 1979), to identify ducting conditions and to assess the effects on various fleet EM emitters. IREPS requires radiosonde data as input.

The disadvantage of IREPS is that it predicts the ducting conditions only at the radiosonde launch site and only at the sounding time. As such, it is not an IREPS weakness but more an inherent weakness in single station assessments. The variability of the atmosphere makes projections in space

and predictions in time of the ducting environment important for the tactician. While satellite data can provide some of the data necessary to make projections in space, something else is needed to predict changes with time. Considering EMCON, the ability to forecast ducting for a 24 hour period may be critical. Under strict EMCON conditions radiosondes cannot be launched because the signal they emit while transmitting data could act like a beacon to hostile forces.

A predictive model exists for changes in the marine atmospheric mixed-layer. The micro computer based model was developed by the Environmental Physics Group at the Naval Postgraduate School (Davidson et al, 1983). The model is initialized with IREPS sounding data, surface observations of sea surface temperature, wind speed, and subsidence at the inversion.

Utilizing the HP-9845 (which all carriers currently have on board for use as part of the IREPS system) and data in IREPS format, Brower (1982) developed a program to incorporate the NPS mixed layer model to predict changes in the refractivity profile for a 30 hour period. The model requires as inputs: surface wind, sea surface temperature, and an estimated subsidence value as well as current IREPS

sounding data to predict the mixed layer evolution and resulting changes in both surface based and elevated duct heights up to 1200 m altitude.

The purpose of this thesis is to evaluate this state of the art atmospheric mixed layer model and its application to fleet tactics. The data utilized in this study were from radiosondes taken by USS NIMITZ and USS CORAL SEA in the Arabian Sea in the vicinity of 23N 061E , a data-poor area, during February 1980.

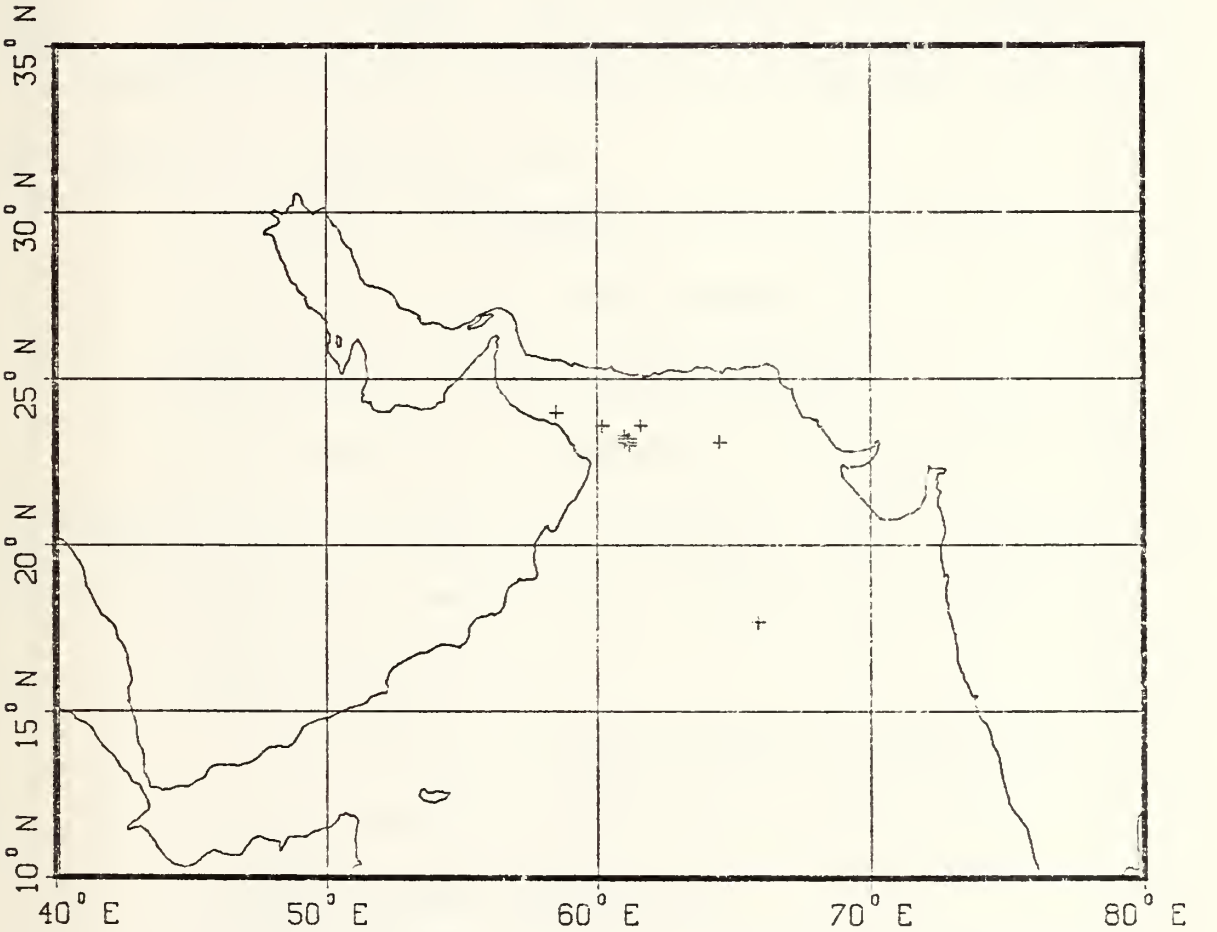

Figure 1. Regional Chart Showing Sounding Data Locations.

II. THE MODEL DESCRIPTION

A. MODEL OVERVIEW

The NPS mixed layer model is an integrated, two layer, zero-order model which predicts changes in the marine atmospheric boundary layer (MABL) below the inversion. The two layers consist of the lower, well-mixed, turbulent boundary layer topped by the relatively non-turbulent free atmosphere. The two layers are separated by an inversion or transition zone which is assumed to have zero thickness. The predicted properties are:

(1) height of inversion

(2) values of well-mixed properties

(3) values of jumps at the inversion

(4) formation of clouds/fog within the mixed layer

Procedural uses are shown in Figure 2, and the equations will be presented in Section B. Inputs to the model are:

(1) Radiosonde data

  (a) Vertical distribution of temperature

  (b) Vertical distribution of moisture

(2) Sea surface temperature

(3) Wind speed

(4) Subsidence

(5) Latitude

(6) Julian date

(7) Local time of sounding

From the predicted properties, a refractivity profile is produced using the refractivity equation (Section B). Observed and predicted sea surface temperature and wind speed are input parameters. Subsidence rates are estimated from previous observations. Latitude, Julian date, and local times are used to estimate incident solar radiation.

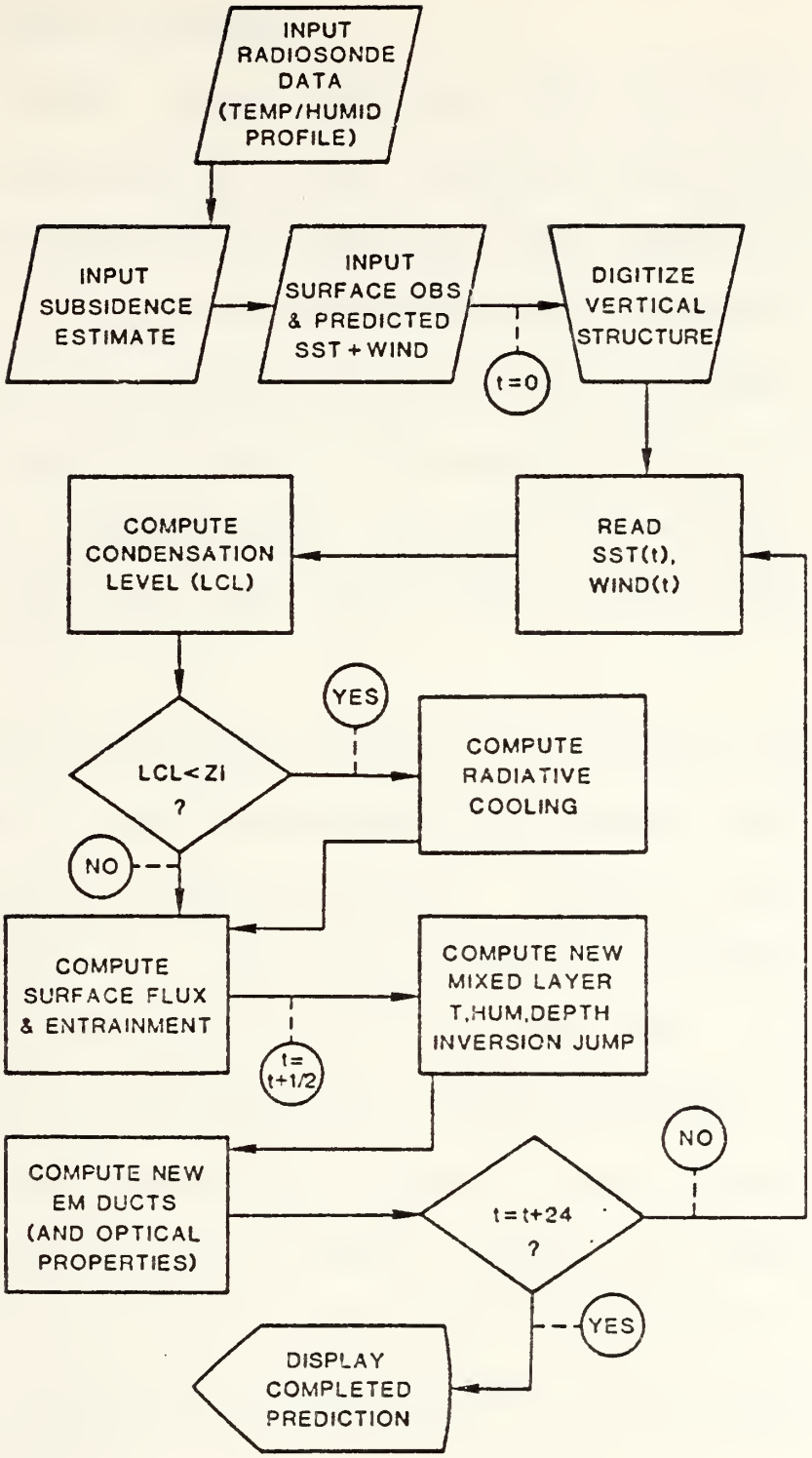

Figure 2. NPS Mixed Layer Model Functional Block Diagram.

B. BASIC MODEL EQUATIONS

Once initial inputs have been made and the vertical structure digitized by fitting straight lines to approximate the vertical profiles of temperature and humidity, Equations 1A, 1B, and 1C are used to calculate the flux scaling parameters. The calculations are based on the air-sea temperature and specific humidity differences and the wind speed. The scaling parameters are then used to estimate surface fluxes of momentum, heat, and moisture in Equations 2A, 2B, and 2C.

Equation 3A is used to predict the change in mixed-layer properties by the difference between surface and inversion fluxes scaled by inversion height. Equation 3B is used to predict changes in the inversion height by adding the flux at the inversion scaled by the inversion jump, a measure of the strength of the inversion, to the subsidence. Equation 3C models the change in the inversion jump by combining the effects of surface and inversion fluxes with subsidence and the change of the inversion height determined in equation 3B. This requires use of the gradient of the property above the inversion.

Flux Scaling Parameters:

$$U^* = C_d^{1/2} U \tag{1A}$$

$$T^* = (\theta - \theta_o)\ C_\theta^{1/2} \tag{1B}$$

$$q^* = C_\theta^{1/2} (q - q_c) \tag{1C}$$

Surface Fluxes:

$$-(\overline{U'W'}) = U^{*2} \tag{2A}$$

$$-(\overline{W'T'}) = U^*T^* \tag{2B}$$

$$-(\overline{W'q'}) = U^*q^* \tag{2C}$$

Where:

C_d, C_θ = stability dependent drag coefficients

U = wind speed

U^*, T^*, q^* = scaling parameters of vertical turbulent momentum, temp. and moisture transfer

$-(\overline{U'W'})$ = downward turbulent transfer of momentum

$-(\overline{W'T'})$ = upward turbulent transfer of heat

$-(\overline{W'q'})$ = upward turbulent transfer of moisture

Predictive Equations (general form):

$$dXm/dt = (\overline{W'X'}c - \overline{W'X'}i + f(R)) / h \tag{3A}$$

$$-\overline{W'X'}i = DX\ (dh/dt - Ws) + f(R) \tag{3B}$$

$$d(DX)/dt = Yx(dh/dt - Ws) - (\overline{W'X'}o - \overline{W'X'}i + f(R))/h \tag{3C}$$

Where:

Xm = any well-mixed property: θ, θv, or q

θ = potential temperature

q = specific humidity

$\overline{W'X'}$ = turbulent vertical transfer (flux) of X

o subscript = "at the surface"

i subscript = "at the inversion"

h = mixed-layer depth (or inversion height)

DX = change in X across the inversion: (Xabove - Xm)

Ws = subsidence at top of inversion

Yx = vertical gradient of X above inversion

f(R) = radiation factor

Refractivity Equation:

$$M = 77.6\ P/T + 6 \times 10^{5}\ (qP/T^{2}) + .157\ Z \qquad (4)$$

Where:

M = modified refractivity

P = atmospheric pressure in millibars

T = temperature in Kelvins

Z = altitude in meters

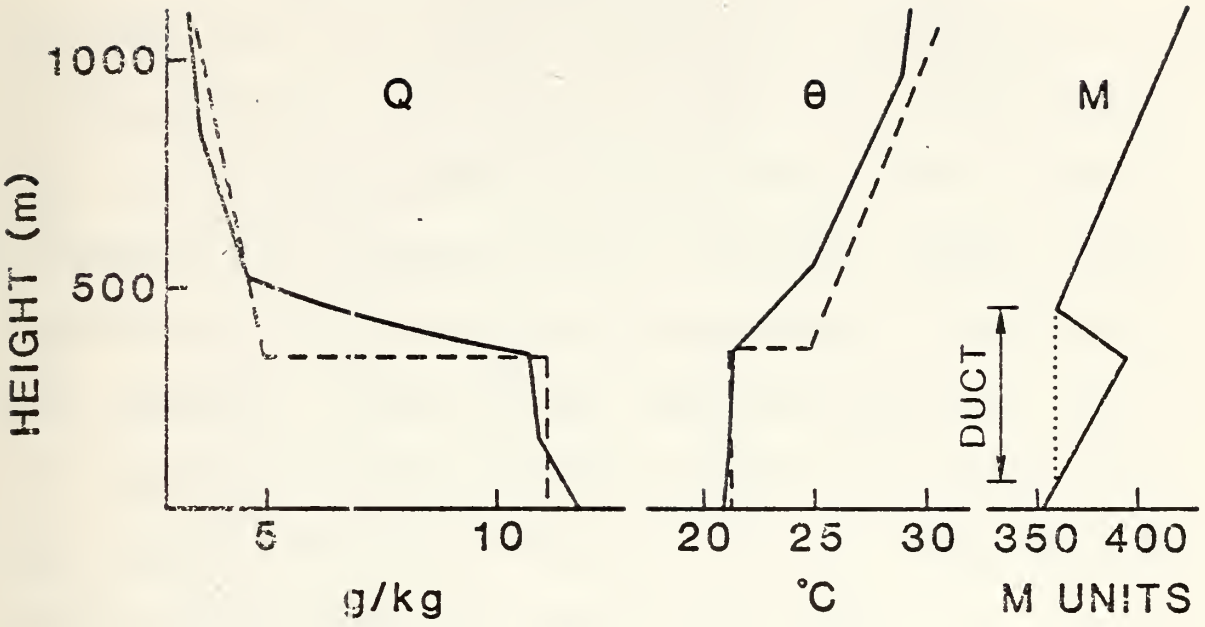

Figure 3. Vertical Structure of θ, q and Corresponding M Profile for a Typical Inversion (Model Simplification is Dashed).

Fig. 3 illustrates the relationship between vertical distribution of temperature and humidity and the modified refractivity, M. M profiles are used as model output because of the ease with which ducting information can be extracted from them. The top of a duct corresponds to the height above the surface where the M value is a minimum. The duct base corresponds to the height at which a vertical line drawn downward from the point of minimum M value first intersects a point of equal M units or the surface.

C. SATELLITE DATA INPUT TO MODEL

Provision is made in the model for incorporating forecast wind and sea surface temperature changes during the prediction period. Although the mixed layer is sensitive to SST, it is believed that accuracies of +/- 1°C in SST are sufficient for reasonable model accuracy. Stewart (1981) reports the following satellite measurement capability has been achieved: NOAA-6 (VHRR) infrared radiometer: SST to .6°C (with no clouds); SeaSat and Nimbus-7 microwave radiometer (SMMR): SST to 1.0°C (with no rain, no RFI (radio frequency interference), and >600 km from land).

Satellite SST could be used in the flux scaling equation (1B) to determine θ_c. Three methods are currently used aboard ship for SST determination: Bathythermographs, sea water injection temperature, and the 'bucket/thermometer' method. None of these yield the actual sea surface "skin" temperature which is the relevant quantity in the determination of stability and turbulent heat and moisture fluxes. Therefore, satellite measurements would not only provide cloud descriptions over broad areas, but would provide a means to obtain the "skin" temperature.

III. ARABIAN SEA CLIMATOLOGY AND SYNOPTIC DESCRIPTION

A. CLIMATOLOGY

The climatology of the northern Arabian Sea is dominated by the summer (southwest) and winter (northeast) monsoons. The data used in this study were from February during the latter part of the northeast monsoon which is characterized by light offshore winds averaging 5-10 knots, and normal Hadley circulation with the subtropical jet located near 30 N at the 200 mb level. Fig. 4 shows the average per cent of time that elevated ducts occur during February to March in this region.

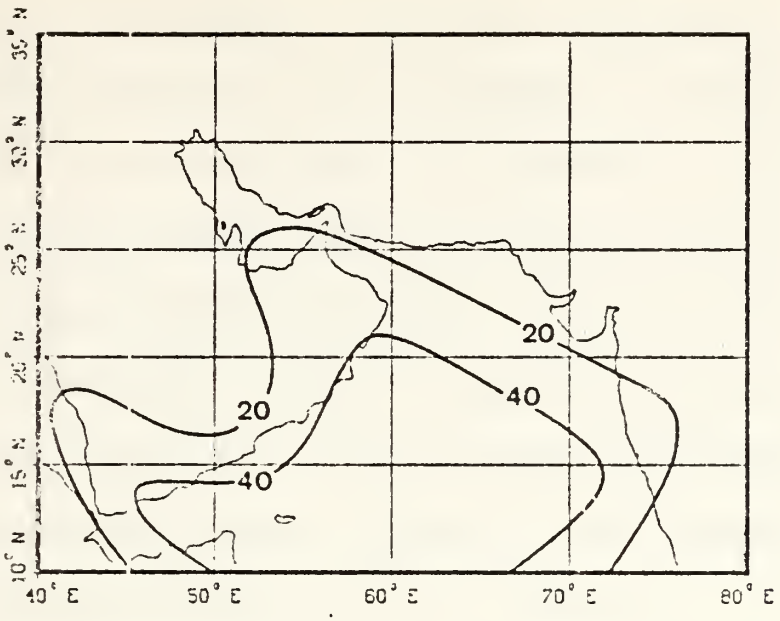

Figure 4. Frequency of Elevated Duct Occurrence During Spring, after Lammers et al (1980).

B. SYNOPTIC CONDITIONS

FNOC (Fleet Numerical Oceanographic Center) products were used to describe the synoptic situation during the data period. They were: Surface Analyses, 500 mb analyses with Temperature fields, 300 mb analyses, 250 mb wind fields. Also, NOAA-6 satellite photos were used to determine cloud coverage of the area as well as to confirm jet positions.

The synoptic situation in the region from 6-23 February 1980 was characterized by a stable high pressure surface ridge over the Arabian peninsula and Arabian Sea, with low pressure troughs over the Red Sea to the west and Indian

subcontinent to the east. The most significant synoptic change occurred from 11 to 14 February as an 850 mb low moved across the northern part of the region. This low was northwest of the Persian Gulf at 30 degrees North latitude on 11 February and tracked eastward, arriving over northern India on 14 February. It was during this brief period of 11-14 February that the minimum shipboard surface pressures for the entire period were recorded. The minimum recorded surface pressure was 1012.0 mb on 14 February.

Table I lists cloud coverage over the immediate area of the data. Low level stratus clouds were confirmed only on 13 February and from 19 to 21 February.

TABLE I

Data Area Cloud Coverage 8-21 February 1980.

DATE	CLOUD TYPE PRESENT
8-11	clear with scattered cirrus
11-12	no satellite coverage
13	low level stratus
14-18	clear with scattered cirrus
19-20	cirrus and stratus
20-21	cirrus, stratus with multilevel to NW

*determined from NOAA 6 IR imagery

An attempt was made to derive subsidence values from synoptic scale wind fields by calculating divergence at various levels. It was noted that at upper levels, wind maxima or jet streams had a dramatic influence on divergence profiles. Although the magnitudes of vertical motion obtained in this manner were inconsistent and highly variable, an interesting and possibly significant observation was made.

The subtropical jet associated with the wind maxima discussed above is usually found at the northern limb of the Hadley Cell (Fig. 5). It is at this northern limb where the greatest downward motion or subsidence is found (Palmen and Newton, 1969). Although this is a feature of the large scale circulation, it seems evident that the jet does have an effect which should be considered in single station assessments whenever possible.

Changes in the subsidence rates calculated by hindcasting and shown in Table II correlated closely with changes in the position and strength of the upper level jet stream. During the period 6-9 February there was a steady decrease in subsidence rates from -.0070 to -.0055 m/s. During the same period the tail of the 250 mb jet max moved steadily eastward from a point due north of the data area. From 6-11

February the 300 mb jet max shifted northward away from the data area.

TABLE II

Calculated Subsidence Rates

RUN	1	2	3	4	5	6	7	8	9
DATE	6-7	6-7	7-8	8-9	8-9	11-12	14-15	21-22	22-23
METHOD									
H	-.30	-.70	-.65	-.60	-.55	-.55	-.75	-.31	-.50
Q	+	-1.72	+	-.39	-.06	-1.17	-.55	-.41	-.33
A	-.54	-.46	-1.10	+	+	-.37	-.33	+	-.50

* subsidence rates in cm/s.
** H hindcast, Q specific humidity, A adiabatic

From 9-12 February, subsidence rates remained at -.0055 m/s. Also, no change in strength or position of the 250 mb jet occurred between 11 and 12 February.

A subsidence rate of -.0075 m/s was determined for the period between 14 and 15 February which was an increase since the 12th. The 300 mb jet strengthened and shifted to the south toward the data area from 12-15 February, and the 250 mb jet increased in strength from 14-15 February.

During the 21-23 February period, subsidence rates increased from -.0031 to -.0050 m/s. During this period,

both the 300 mb and the 250 mb jet maxima moved closer to the data area with the 300 mb jet strengthening and the 250 mb jet weakening.

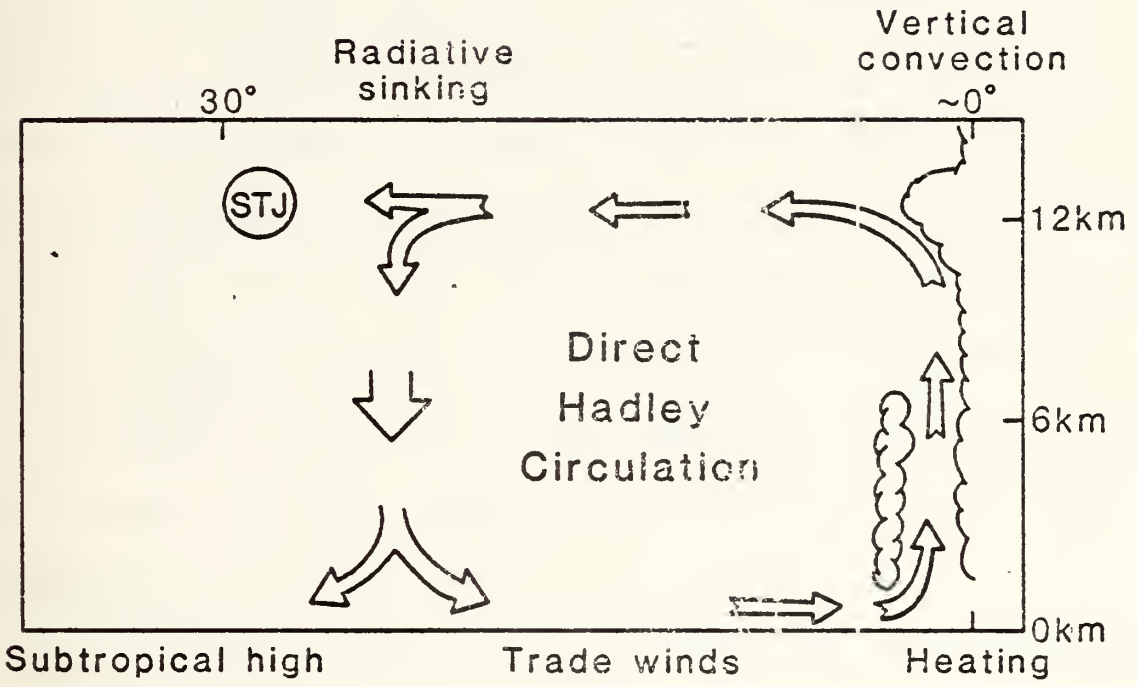

Figure 5. Hadley Cell and Subtropical Jet Position Showing Area of Maximum Downward Motion, after Palmen and Newton (1969).

IV. THE MODEL PERFORMANCE

A. DUCT PREDICTION

Each sounding was run with IREPS to establish a baseline to assess the model's ability to predict changes in ducting conditions. It was then possible to compare the model predicted duct heights with those observed. Seven different pairs of soundings were examined, with each pair separated by 24 hours. Two of the 24 hour periods had 2 simultaneous, spatially separated soundings at the end of the periods. On one occaision, one of the second soundings was taken at a location 425 nautical miles to the southeast of the first sounding.

The observed winds at the start and end of the period were used and interpolated linearly within the period to specify the wind for the prediction period. Sea surface temperature at the latitude and longitude of the initial sounding and at the latitude and longitude of the verifying sounding were also interpolated within the period.

Subsidence velocities were determined by hindcasting such that the predicted inversion height agreed with that

observed in the verifying sounding. Predicted ducts using this "hindcast" subsidence are compared with IREPS observed ducts in Table III . The RMS errors of the model are approximately one half the errors of persistence. Persistence is considered to be a "prediction" of no change. It is frequently used as a baseline against which predictions are compared to determine if the predictive method has merit. These results indicate that when subsidence can be accurately estimated, the model's performance is clearly superior to persistence in predicting duct bases and tops.

TABLE III

Comparison of Observed Duct Heights With Model Predicted Heights Using Hindcast Subsidence Values.

RUN NUMBER	INITIAL SOUNDING	VERIFYING SOUNDING	MODEL PREDICTION
1	788-983	470-877	345-740
2	788-983	633-988	500-960
3	470-877	46-504	0-370
4	47-504	0-135	0-170
5	47-504	0-304	0-158
6	no duct	5-584	115-375
7	723-1031 and 0-112	248-569	0-495
8	206-503	no duct	50-420
9	no duct	0-258	0-250

RMS ERRORS:	PREDICTION	PERSISTENCE
TOP	178	364
BASE	111	214
THICKNESS	185	285

* heights in meters.

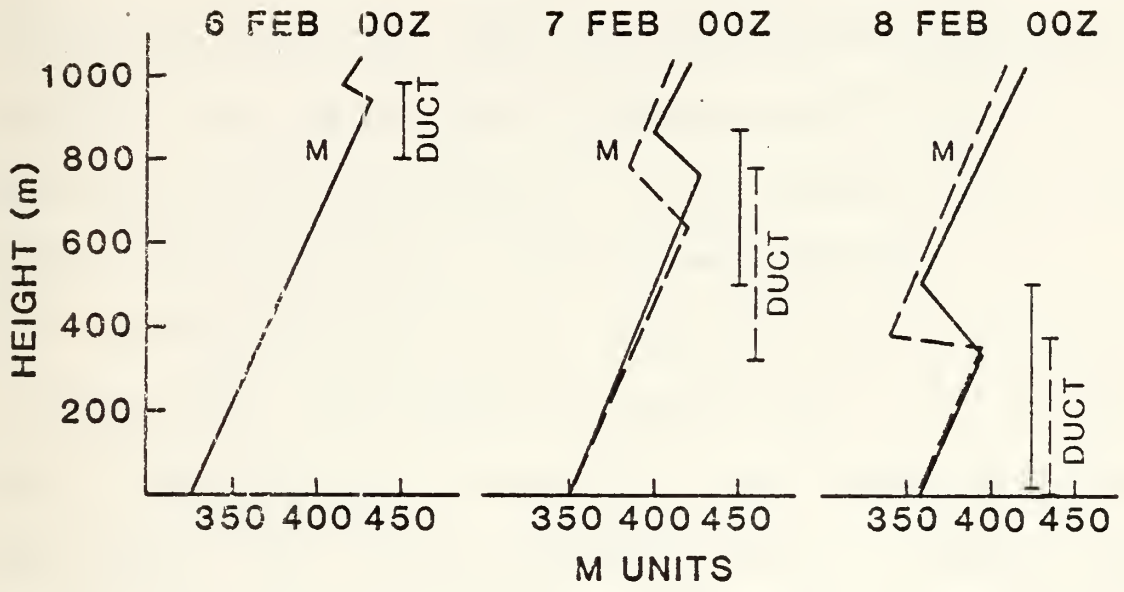

Figure 6. Model Predicted Ducts (dashed) vs. Observed Ducts (solid) for the Period 6-8 February 1980.

For a true predictive application, at least 3 sequential soundings are required. The first and second sounding enable the estimation of subsidence. The model is then initiated from the second sounding using the subsidence obtained from the first and second. The third sounding is used to verify the prediction. Gleason (1982) found that a method which is based on the well mixed specific humidity is an accurate method to calculate subsidence. However, assuming persisterce in subsidence rates appears to be the best.

A steady decrease in subsidence rates (Table II) during the first week of the data period coincided with a steady decrease in surface pressure. The upper level jet stream shifted away from the data area and weakened during this period. This suggests that judicious modification of persistence-obtained subsidence may be appropriate in some cases especially when a trend has been observed.

From three periods having 3 sequential soundings, Tables IV and V show the results of predictions. In the first period (Run number 3), an elevated layer became nearly surface based. The model prediction was for a surface based duct. In the second period (Run number 4), a low elevated duct became surface based. The model prediction matched the observation nearly perfectly. In the third case (Run number 9), a surface based duct formed when there was no duct initially. In this case, the model predicted the formation of an elevated duct. While the predicted duct in the third case differed substantially in both height and thickness from the observed duct, the model prediction was significant because the occurance of a duct was predicted from an initial non-ducting condition.

For this particular comparison, the absolute errors are more meaningful than rms errors. Two of three model predictions are essentially on the mark while all of the error is concentrated in the third. In the persistence cases, the errors are fairly evenly distributed.

TABLE IV

Comparison of Observed Ducts with Model Predicted Ducts Assuming Persistent Subsidence.

RUN NUMBER	INITIAL SOUNDING	VERIFYING SOUNDING	MODEL PREDICTION
3	470-877	46-504	0-350
4	46-504	0-135	0-140
9	no duct	0-258	490-820

* heights in meters.

TABLE V

Error Analysis of Model Prediction vs. Persistence.

RUN		ABSOLUTE ERROR MODEL	ABSOLUTE ERROR PERSISTENCE	3 RUN RMS ERROR MODEL	3 RUN RMS ERROR PERSISTENCE
3	TOP	154	373	336	337
	BASE	46	424	284	246
	THICKNESS	108	51	75	240
4	TOP	5	369		
	BASE	0	47		
	THICKNESS	5	323		
9	TOP	562	258		
	BASE	490	0		
	THICKNESS	72	258		

* heights in meters.

B. CLOUD PREDICTION

The cloud formation is predicted on the basis of concurrent prediction of the lifting condensation level (LCL) and the inversion height. If the LCL is below the inversion, clouds occur; if it is above, no clouds occur. When model predictions showed no low level clouds forming, satellite imagery confirmed there were no low level clouds and that the sounding site either was clear or showed scattered high cirrus clouds. The formation of low level stratus clouds was predicted on 3 occasions over the entire period. Stratus clouds were predicted to form at 2100 local time 11 February. The first satellite imagery available following this time was at 0800 13 February, and showed the presence of low level stratus clouds (Fig. 8).

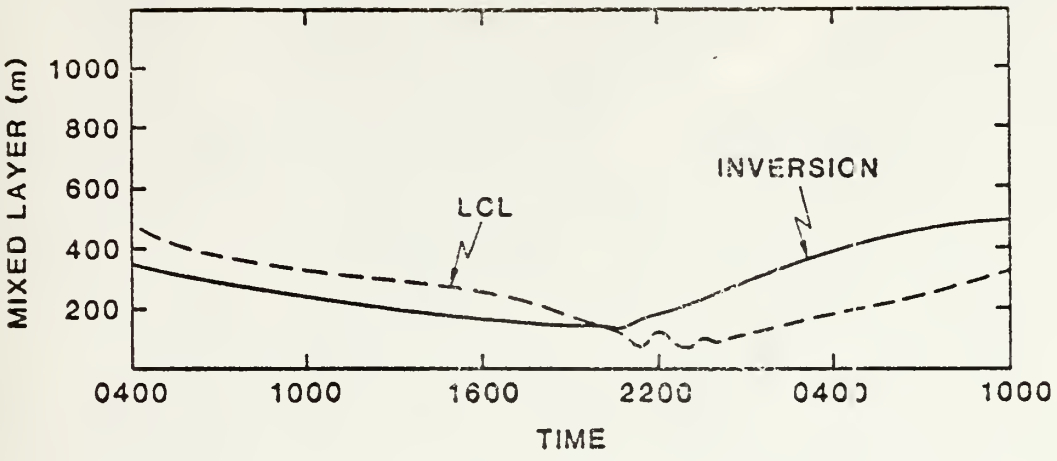

Figure 7. Model Prediction Showing LCL Dropping Beneath the Inversion at 2100 11 Feb.

Clouds were predicted to form at 0500 15 February (25 hours into the 30 hour prediction). In this case the LCL dropped slightly below the inversion, but less sharply than in the other cases. Satellite imagery from 15 February shows no clouds (Fig. 10).

Satellite imagery shows the presence of low level stratus clouds on the 2000 pass 19 February and increased amounts on the 0800 20 February pass. Although no soundings were available to initialize the model prior to this initial formation of clouds, on the next available model run clouds were predicted throughout the period 0700 21 February to 0700 22 February. Satellite imagery confirm the presence of

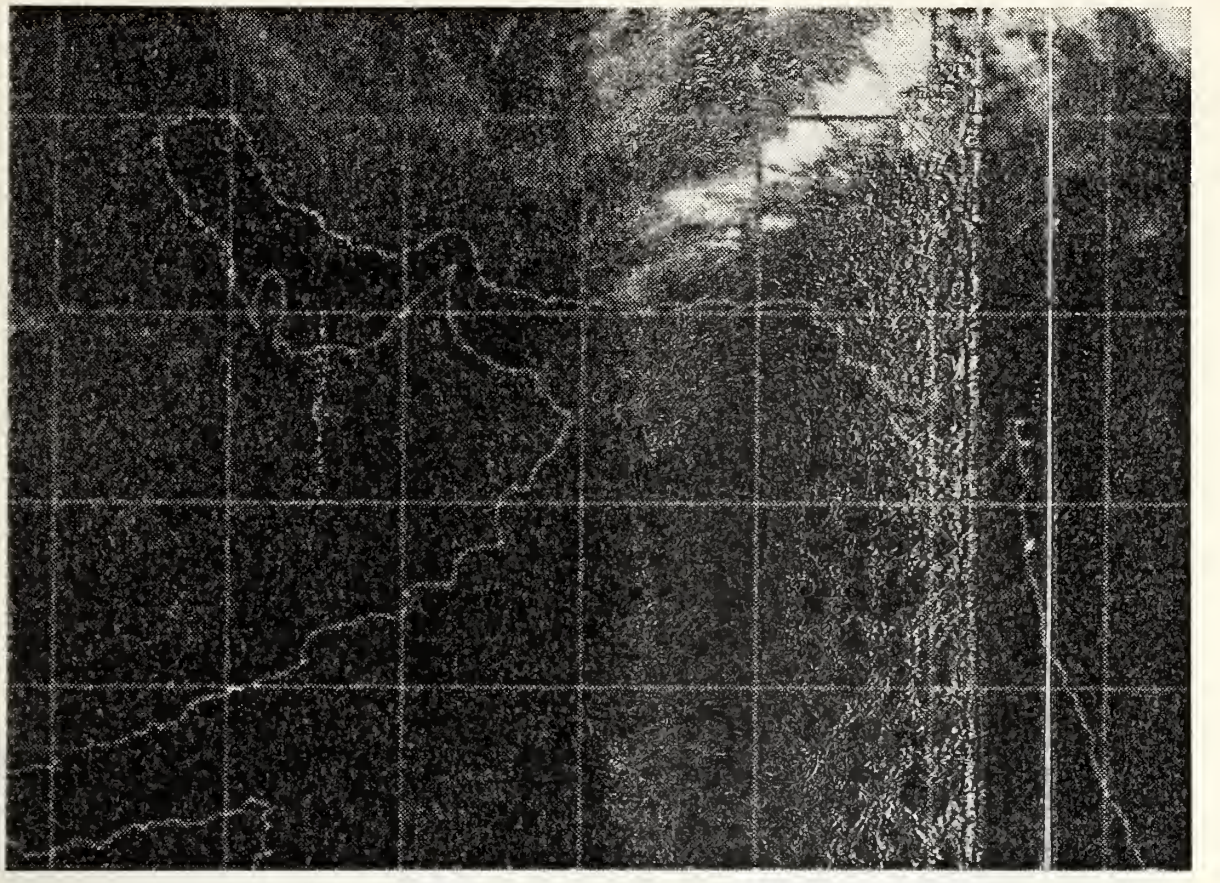

Figure 8. NOAA 6 Satellite IR Imagery from 0800 13 February Showing the Presence of Stratus Clouds.

both cirrus and stratus clouds on both the 0800 and 2000 passes on 21 February (Fig. 12).

Although the satellite imagery analysis was by necessity, subjective, some objectivety was retained by confirming the initial analysis with a second analysis by an independent source. Both analyses agreed on cloud types. Since the model could be shown to be incorrect only on one occasion, the model's overall performance in predicting the

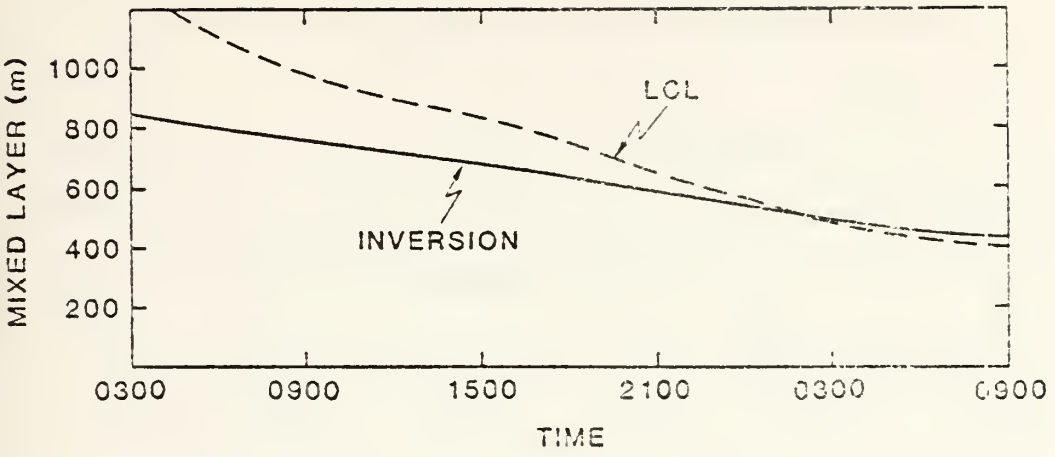

Figure 9. Model Prediction 0300 14 to 0900 15 February.

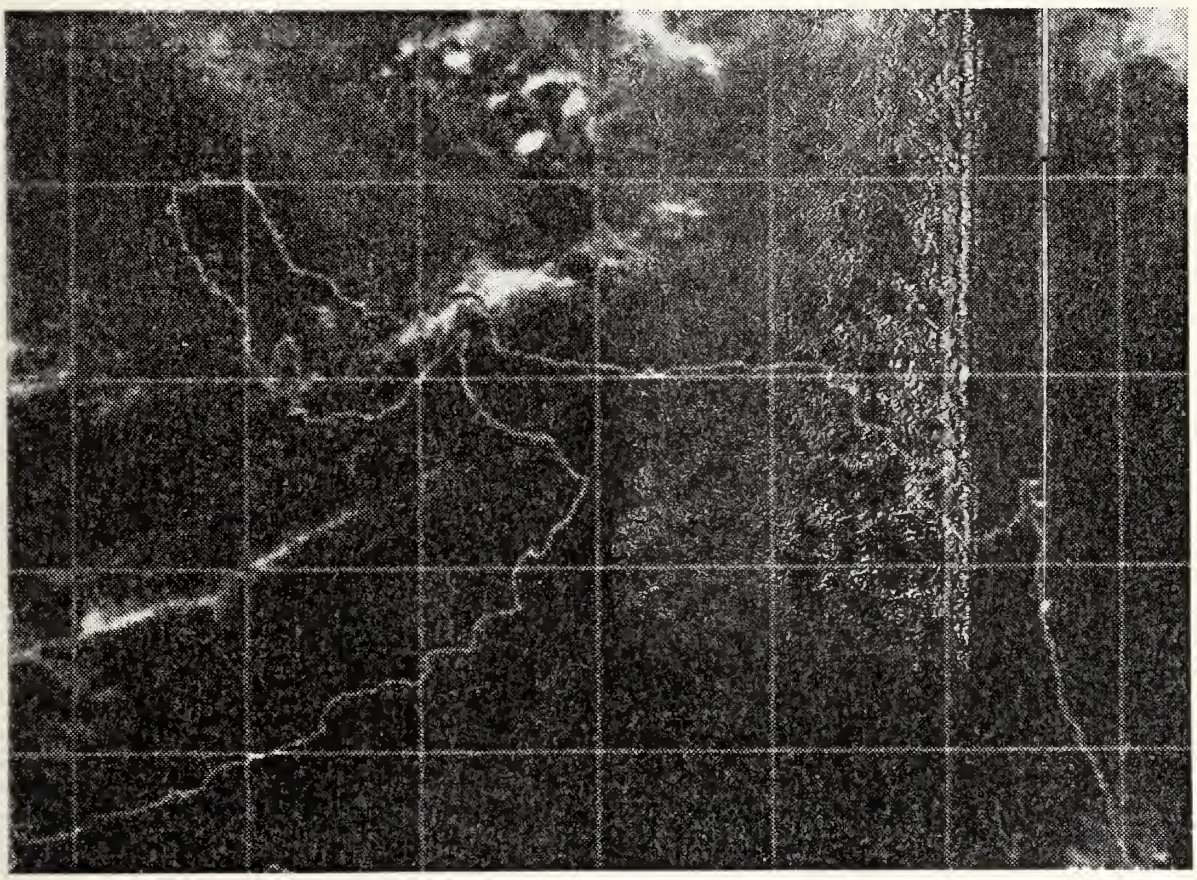

Figure 10. NOAA 6 Satellite IR Imagery from 15 February.

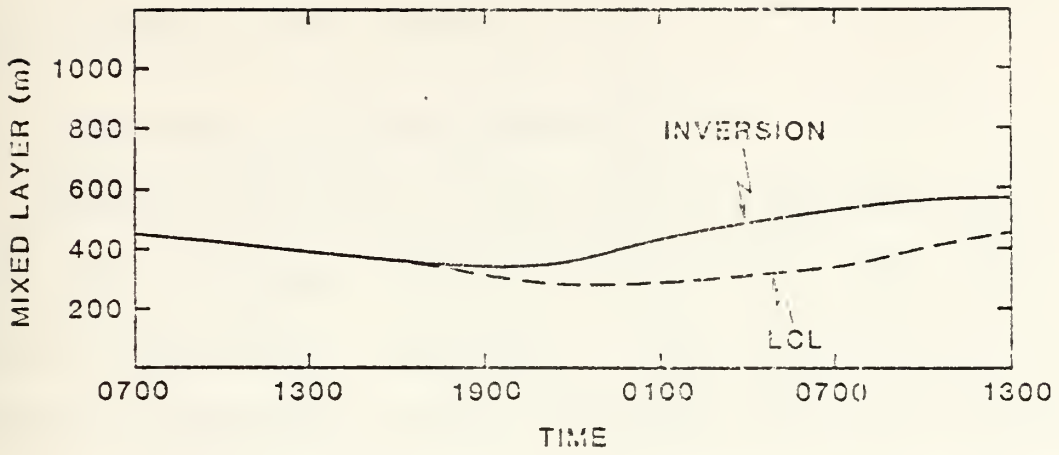

Figure 11. Model Prediction 0700 21 to 1300 22 February.

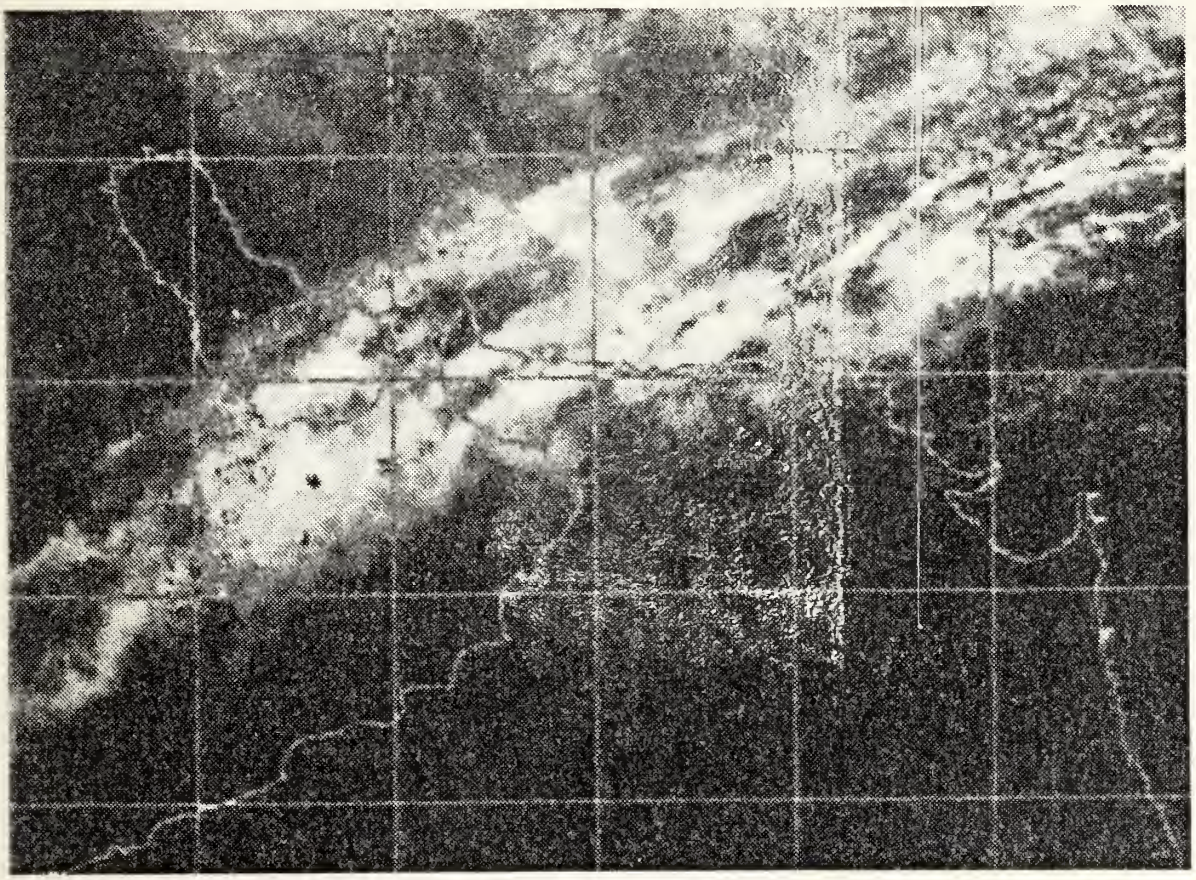

Figure 12. NOAA 6 Satellite IR Imagery 0800 21 February.

formation of low level clouds/fog was eight out of nine cases correct or 89% correct.

C. EXAMINATION OF MODEL SENSITIVITY

Surface observation of sea surface temperature (SST) and wind can be obtained with an accuracy of +/- 1°C and +/- 2 knots respectively. To test the model sensitivity to these possible measurement errors, successive model runs were made with SST 1°C higher and lower than observed. The effect of wind measurement error was evaluated using wind values 2 knots higher than observed. The resulting duct predictions were then compared with ducts predicted by actual observed winds and SSTs. Table VI contains the tabulated results. Noting that RMS error in duct specifications due to potential SST measurement error are approximately double the RMS error due to potential wind measurement error, one might reasonably conclude SST determination is the more critical of the two parameters. It is imperative to recognize that the wind has a much wider range of variability than the SST and accurate specification of both parameters are important for good model performance.

TABLE VI

Sensitivity of Model Duct Predictions to SST and Wind Variations.

RUN NUMBER	VERIFYING DUCTS	SST +1°C	SST -1°C	WIND +2 KTS	WIND -2 KTS
1	345-740	400-800	315-715	390-810	330-725
2	500-960	780-1190	420-870	625-1080	545-975
3	0-370	0-395	0-360	0-400	0-365
4	0-170	0-270	0-110	0-180	0-140
5	0-158	0-210	0-115	0-170	0-130
6	115-375	170-570	0-80	25-310	0-240
7	0-495	290-430	0-440	0-510	0-450
8	50-420	0-360	0-310	70-450	0-370
9	0-250	0-240	0-290	0-240	0-190

Combined RMS error:	SST	DUCT	WIND
	114	top	55
	104	base	50
	107	thickness	26

* heights in meters.

The model's demonstrated sensitivity to sea surface temperature points to the need for accurate SST determinations. Current methods to measure sea surface temperature include: monitoring sea water injection temperature (20-40 ft. beneath the surface); utilizing BT drops (get temperature at about 1 ft.); and the bucket and thermometer method (get temperature of top few inches). None of these methods yield the sea surface skin temperature which is the quantity necessary to determine the surface fluxes. These fluxes, in turn, drive the evolution of the mixed layer, the inversion, and thus ducting conditions of the lower atmosphere.

The 052340Z February 1980 sounding was used to test model sensitivity to varying subsidence rates. The hindcast subsidence was -.0030 m/s (Table II) which resulted in a predicted 395 meter thick elevated duct with the top at 740 meters elevation and the base at 345 meters. Subsidence was varied from this baseline value and deviations in the predicted duct height and thickness were recorded. This particular sounding was chosen because the associated initial and verifying ducts were elevated, which allowed the varied subsidence to affect the position of the predicted duct in both the upward and downward directions.

Deviations in the duct predictions resulting from subsidence specification errors of +/- .0030 m/s are 245 m at the top, 269 m at the base, and 25 m in thickness (Table VII). Errors resulting from assuming persistence in duct heights (Table III) are approximately equal to the errors resulting from a subsidence specification error of +/- .0030 m/s. From this single case comparison, it is clear that the model is an improvement over persistence only when subsidence can be specified to within +/- .0030 m/s.

The range of subsidence calculated during the short period from 6 to 22 February 1980 in the data area was

-.0030 to -.0075 m/s or -.00525 +/- .00225 m/s. Assuming this to be a normal range of variability and the median value, -.00525 m/s, to be representative of the climatological subsidence, then the "climatological" value appears to be less than the +/-.0030 m/s marginal utility criterion. This conclusion, based on a limited data set, seems to indicate that a climatological subsidence value would provide a duct height forecast which, on the average, has some skill over persistence or a forecast of no change.

In reality, errors will not be confined to subsidence alone, but will be caused by errors in other inputs such as wind and SST. While SST, wind, and subsidence errors may be offsetting at times, there will be times when they will be additive. When all the errors are additive, the expected duct height error for SST plus wind measurement errors are 169 m at the top and 154 m at the bottom (Table V). Given the errors due to assuming persistence in duct heights of 364 m at the top and 214 m at the base of the duct (Table IV), the difference of approximately 200 m at the top and 60 m at the base indicate the maximum duct height error permissible due to subsidence specification error is, in the mean, 130 m. From Table VI, the subsidence specification error

expected to produce this 130 m duct height error is approximately +/- .0015 m/s.

From the cases (Table III) in which the best possible estimate of subsidence, the hindcast value, was used, the RMS model prediction error averages 143 m less than persistence error. It will be shown later that if subsidence is allowed to vary from this "best estimate", a deviation of about +/- .0017 m/s will produce the additional 143 m error in height of duct top and base necessary to render the prediction no better than persistence.

In conclusion, evaluations of the model with the data indicate that with the expected SST and wind measurement errors, subsidence must be specified to within +/- .0015 m/s for the model to consistently outperform persistence. The observed range of subsidence variablity from this limited data set of +/- .00225 m/s effectively rules out the use of a climatological subsidence as a viable input parameter.

TABLE VII

Sensitivity of Model Duct Predictions to Subsidence.

SUBSIDENCE (m/s)		PREDICTED DUCT PARAMETERS TOP	CHANGE	BASE	CHANGE	THICKNESS	CHANGE
.0000		1020	280	645	300	375	-20
-.0005		970	230	585	240	385	-10
-.0010		910	170	535	190	375	-20
-.0015		865	125	480	135	385	-10
-.0020		830	90	430	85	400	5
-.0025		785	45	380	35	405	10
-.0030	*	740	0	345	0	395	0
-.0035		713	-27	312	-33	401	6
-.0040		675	-65	260	-85	415	20
-.0045		630	-110	225	-120	405	10
-.0050		600	-140	180	-165	420	25
-.0055		570	-170	145	-200	425	30
-.0060		535	-205	110	-235	425	30

RMS ERRORS:

SUBSIDENCE	DEVIATION FROM REFERENCE TOP	BASE	THICKNESS	EXPECTED DEVIATION (Ws X 24 hours)
+/- .0030	245	269	25	259
+/- .0025	202	221	22	216
+/- .0020	156	178	23	173
+/- .0015	118	128	10	130
+/- .0010	79	85	15	86
+/- .0005	37	34	8	43

* reference values
** heights in meters

V. TACTICAL APPLICATIONS

The first consideration in tactical application of the model is the recognition of its capabilities and limitations. It can be used to estimate when low clouds or fog can be expected to form. It can be used to estimate the expected position of low elevated and surface based ducts below 1200 m over an 18 - 24 hour period. However, it cannot predict information on upper level ducts.

The tactical significance of knowing up to 30 hours in advance that visibility may be reduced or a low ceiling developed will depend on current and planned operations. The results presented in Chapter IV B indicate that the model does well in predicting low level stratus/fog.

When fog or low level stratus clouds are predicted, the following possible effects on own and enemy forces in each warfare area should be considered:

(1) maneuverability restricted

(2) lost or reduced visual signalling capability

(3) reduced visual target detection/identification

(4) degraded optical equipment performance including IR weapons and sensors

(5) hampered flight operations for carrier based

aircraft and LAMPS

Tactical employment of Naval assets requires a knowledge of the state of the environment if those assets are to be employed effectively. To that end, IREPS (Integrated Refractive Effects Prediction System) was developed. When radiosonde data are input to IREPS, a refractivity profile is generated which is utilized to define the location of ducts and to assess radar coverage, ESM and communication ranges.

Because soundings are normally taken only once or twice daily from aircraft carriers and the atmospheric boundary layer undergoes change, there exists a need to be able to predict changes in the refractivity profile between soundings. This prediction can be critically important to battle groups in the positioning of both surface and air assets, and in the intelligent management of the EMCON plan.

The duct prediction capability, as detailed in Chapter IV A, provides a significant planning tool. Tactical useage of the duct predictions stems from the effects of ducts on EM propagation. Prediction of a surface based duct indicates probable extended ranges for transmitter-receiver antenna pairs in the duct and possible holes or gaps in

coverage just above the duct for antennas in, near, or below the duct.

The predicted M profile may be used as an environmental data set to run IREPS and coverage diagrams generated for specific emitters. This procedure was used with a hypothetical surface search radar under observed refractive conditions and model predicted refractive conditions. IREPS version 1.7 (unclassified) was used to generate the coverage diagrams. Radar parameters for the hypothetical radar were: Antenna height 110 ft., antenna type sin(x)/x, vertical beam width 10°, elevation angle 0°, free space range 55 nautical miles, and frequency 5 Ghz.

Clearly shown in Figs. 14 and 15 is the model's value in predicting the occurance of low level ducts. The radar coverage in Fig. 14 is significant in that the initial propagation conditions were for surface target detections out to about 25 nm and the predicted conditions were for detections well in excess of 100 nm. The predicted propagation conditions were in close agreement with those observed.

An example of how the model might be used operationally is as follows:

(1) radiosonde is launched and surface observations of SST and wind are recorded.

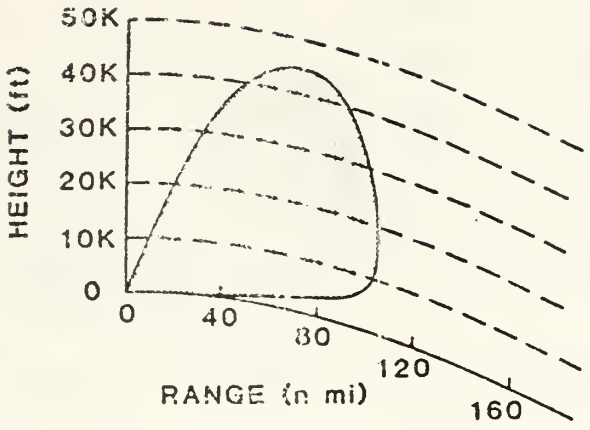

Figure 13. Initial Surface Search Radar Coverage 0420 7 Feb 80.

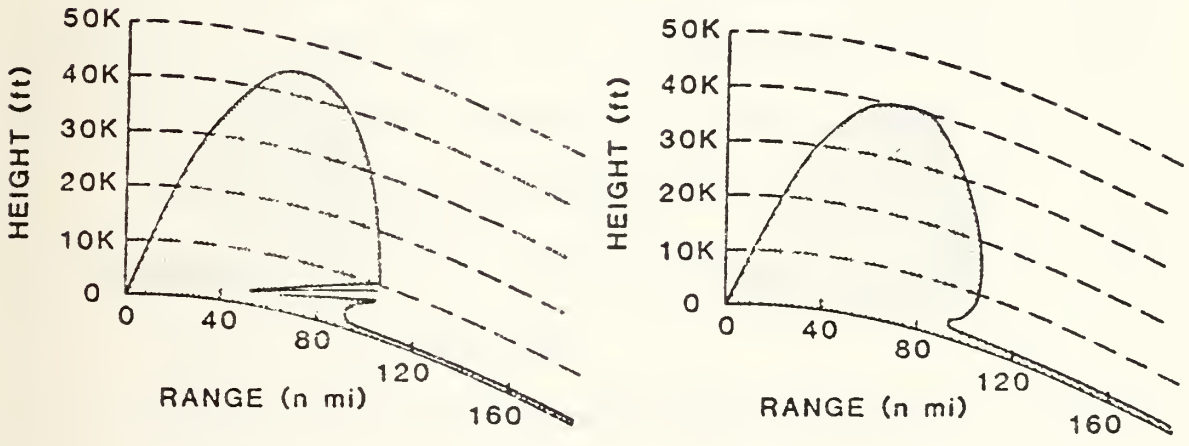

Figure 14. Surface Search Radar Coverage 0333 8 Feb 80 Based on Actual Sounding (l) and Model Prediction (r).

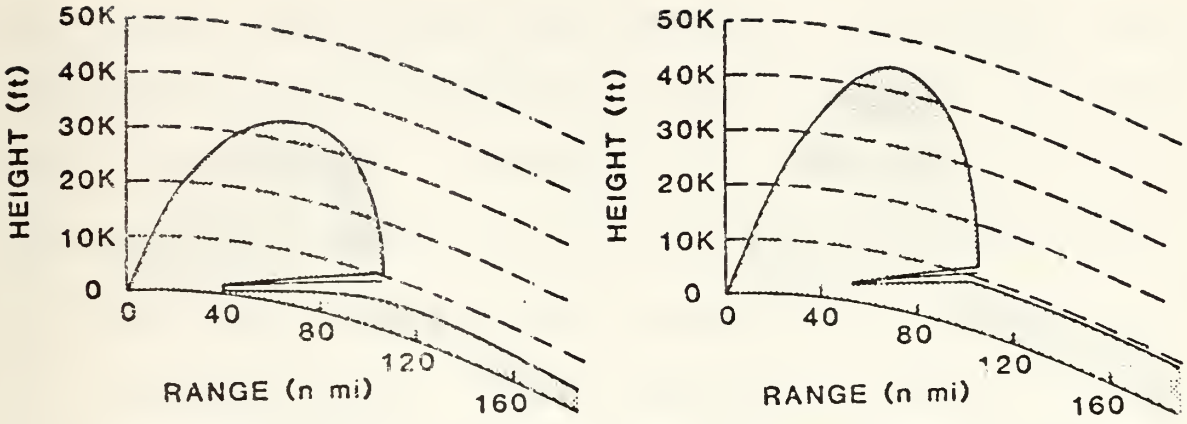

Figure 15. Surface Search Radar Coverage 0240 9 Feb 80 Based on Actual Sounding (l) and Model Prediction (r).

(2) radiosonde data are input to IREPS and coverage diagrams are generated to make current assessments.

(3) radiosonde data and surface observations are input to the NPS model and a 30 hour prediction is made.

(4) the predicted M profile is input to IREPS and predicted coverage diagrams are generated.

(5) operational plans, incorporating forecast ducting effects, are proposed.

(6) tactical decisions, using the environment to the advantage of the force, are made.

In a scenario similar to that observed in the Arabian Sea 7 to 9 February 1980 when an elevated duct became surface based, many tactical considerations are involved. Suppose the battle group wanted to avoid detection by an enemy force in the region. Forewarned that surface based ducting was expected to occur in 12 to 18 hours and that UHF radio transmissions, normally useful between ships only up to 25 to 30 nautical miles, could be detected at ranges in excess of 200 nautical miles due to ducting, the battle group commander would be able to impose a more restrictive EMCON condition in adequate time to prevent hostile intercept of the group's transmissions. Alternatively, if the battle group commander expected to be opposed by active surface search radar, he could: initiate a preemptive attack before his presence was exposed; steam out of range; or, relax EMCON at the appropriate time.

For a battle group in a multithreat environment, early threat detection is critical to defeat the threat at minimum cost to the battle group's offensive capability. The 12 to 18 hour advance notice of surface based ducting provides the tactical planner the tool necessary to use his limited surveillance assets with the efficiency needed for sustained

operations and the effectiveness required for early threat detection. Surface ships could be positioned in such a way as to take maximum advantage of the extended surface search radar ranges afforded by the surface based duct. Airborne surveillance assets, freed from task of surface surveillance, could concentrate their efforts toward detecting and tracking air targets. The net result is increased force effectiveness. Depending on the battle group's speed and the picket station assigned, the surface ship may require several hours to reach the assigned station, thus making the lead time provided by the prediction all the more important.

The timing of war at sea strikes to coincide with predicted occurrence of a surface based duct could give considerable advantage to the strike aircraft by enabling them to use predicted holes just above the duct to penetrate enemy surveillance and to use the duct for targeting and jamming. In such a case, a 12 to 18 hour prediction provides time to plan mission tactics, arm aircraft, and conduct mission briefs.

When sonobuoy patterns are laid and monitored by LAMPS, one constraint on placement of the bouys is LAMPS' on station endurance. When a surface based duct occurs, sonobouys

can be monitored at greater distances. Prediction in advance of surface based ducting provides the lead time necessary to plan and lay bouy patterns at distances from the battle group which take advantage of the extended monitoring range.

VI. CONCLUSIONS AND RECOMMENDATIONS

The Tactical Environmental Support System (TESS), currently under development, will incorporate various satellite derived products, and single station assessment systems such as IREPS and the NPS mixed layer model. This will place state of the art environmental sensing and predictive capability at the disposal of those who need the information: the operational commanders.

Based on evaluations with a limited data set, the NPS model has been demonstrated to perform well both in predictions of low level cloud formation and in predictions of low elevated and surface based ducts. Further work is required to determine the model's range of applicability both geographically and seasonally. It is believed that when subsidence can be specified with an accuracy of +/-.0015 m/s, the model can be used to accurately forecast low level ducts. Two additional recommendations are detailed in the following paragraphs.

In tactical situations where the outcome may depend on accuracy of duct predictions, a method is needed to verify

the prediction. A radiosonde launch may be impractical due to EMCON conditions. An acoustic sounder can be used to measure the height of the inversion which, as shown in Fig. 3, corresponds to the top of the duct. Davidson , et al (1982), while conducting marine atmospheric boundary layer research, utilized the economical acoustic sounder on R. V. ACANIA to monitor inversion height. Using a combination of daily radiosondes, NPS model duct predictions, and periodic acoustic soundings to track the inversion height would provide improved capability to use the environment. It is therefore recommended that similar acoustic sounders be installed on aircraft carriers.

Determining appropriate temperature and humidity profiles during initialization of the model is a possible source of error. There are two schools of thought which differ on the appropriate height for the inversion initialization. Sounding data typically show the inversion as a layer 100 to 200 meters thick, while the model requires a single height to be specified. One school suggests that the bottom of the inversion layer is best while the second suggests that the midpoint of the layer is most reasonable.

The work in this thesis used the former method. The model predictions (Table III) show a bias in that nearly all of the predicted duct heights are lower than those observed. This seems to indicate that inversion heights should be digitized at the midpoint of the layer instead of at the bottom. It is recommended that further work be done in this area to establish a more objective method of digitization.

The NPS atmospheric boundary layer model could provide the fleet a predictive capability and tactical planning tool. Consideration should be given to introducing it into the fleet for operational evaluation. The need to understand the model assumptions in order to assess model applicability in a given environmental situation, the need for accurate subsidence estimates, and the requirement for surface wind predictions preclude model installation except where qualified personnel are assigned. In this regard, the model should be installed at locations (aircraft carriers) where there are Geophysics Officers who can interpret and use the model as a tool along with other meteorological information.

APPENDIX A

RADIOSONDE TIMES AND LOCATIONS

TABLE VIII

Radiosonde Data Set.

SOUNDING	SHIP	DTG	LATITUDE	LONGITUDE
1	NIMITZ	052340Z	23°12'N	061°09'E
2	NIMITZ	070020Z	22°38'N	061°36'E
3	CORAL SEA	070030Z	17°40'N	065°51'E
4	NIMITZ	072333Z	23°07'N	061°00'E
5	CORAL SEA	082240Z	23°00'N	061°11'E
6	NIMITZ	082333Z	23°13'N	061°00'E
7	NIMITZ	110014Z	23°17'N	060°59'E
8	NIMITZ	112346Z	23°10'N	061°01'E
9	NIMITZ	132307Z	23°03'N	064°30'E
10	NIMITZ	150013Z	23°11'N	061°07'E
11	NIMITZ	210300Z	24°01'N	058°32'E
12	CORAL SEA	212035Z	23°06'N	061°12'E
13	NIMITZ	212244Z	23°18'N	060°58'E
14	CORAL SEA	222015Z	23°38'N	060°09'E

* date-time groups February 1980

TABLE IX

Radiosondes Used in Model Performance Runs.

RUN NUMBER	1	2	3	4	5	6	7	8	9
SOUNDINGS:									
INITIAL	1	1	2	4	4	7	9	11	12
VERIFYING	2	3	4	5	6	8	10	12	14

LIST OF REFERENCES

Brower, D. A., 1982: Marine Atmospheric Boundary Layer and Inversion Forcast Model, M. S. Thesis, Naval Postraduate School, Monterey, CA., 134 pp.

Davidson, K. L., G. E. Schacher, C. W. Fairall, P. Jones Boyle, and D. A. Brower, 1982: Marine Atmospheric Boundary Layer Modeling for Tactical Use, NPS-63-82-001, Naval Postgraduate School, Monterey, CA., 80 pp.

Davidson, K. L., C. W. Fairall, P. J. Boyle, and G. E. Schacher, 1983: Verification of an Atmospheric Mixed-Layer Model for a Coastal Region, J. Appl. Meteor., (submitted).

Gleason, J. P., 1982: Single Station Assessments of the Synoptic Scale Forcing on the MarineAtmospheric Boundary Layer, M. S. Thesis, Naval Postgraduate School, Monterey, CA., 57 pp.

Hitney, H. V., 1979: Integrated Refractive Effects Prdiction System (IREPS) and Environment/Weapons Effects Prediction System (E/WEPS), paper presented at the Conference on Atmospheric Refractive Effects Assessment, San Diego, California, 23 January 1979, 13-17.

Lammers, U. H. W., J. T. Doherty, and R. A. Marr, 1980: Anomolous Tropospheric Refraction Near the Arabian Peninsula, RADC-TR-80-216, Rome Air Development Center, 63 pp.

Nash, J. R., 1976: Darkest Hours, Nelson-Hall, 812 pp.

Palmen, E. and C. W. Newton, 1969: Atmospheric Circulation Systems, Academic Press, 603 pp.

Stewart, R.H., 1981: Satellite Oceanography: the Instruments, Oceanus, 24, 3, pp. 66-74.

INITIAL DISTRIBUTION LIST

		No. Copies
1.	Defense Technical Information Center Cameron Station Alexandria, VA 22314	2
2.	Library, Code 0142 Naval Postgraduate School Monterey, CA 93940	2
3.	Professor Robert J. Renard, Code 63Rd Department of Meteorology Naval Postgraduate School Monterey, CA 93940	1
4.	Professor Christopher N. K. Mooers, Code 68Mr Department of Oceanography Naval Postgraduate School Monterey, CA 93940	1
5.	Professor Kenneth L. Davidson, Code 63Ds Department of Meteorology Naval Postgraduate School Monterey, CA 93940	10
6.	Capt. Wayne P. Hughes, Code 55Hl Department of Operations Research Naval Postgraduate School Monterey, CA 93940	1
7.	Lt. Ronald M. Graves U.S.N. Department Head Course, Class 77 SWOSCOLCOM Bldg. 446 Newport, Rhode Island 02840	1
8.	Director Naval Oceanography Division Naval Observatory 34th and Massachusetts Avenue NW Washington, D.C. 20390	1
9.	Commander Naval Oceanography Command Central NSTL Station Bay ST. Louis, MS 39522	1
10.	Commanding Officer Naval Oceanographic Office NSTL Station Bay St. Louis, MS 39522	1

11. Commanding Officer 1
Fleet Numerical Oceanography Center
Monterey, CA 93940

12. Commanding Officer 1
Naval Ocean Research and Development
Activity
NSTL Station
Bay ST. Louis, MS 39522

13. Commanding Officer 1
Naval Environmental Prediction Research
Facility
Monterey, CA 93940

14. Chairman, Oceanography Department 1
U.S. Naval Academy
Annapolis, MD 21402

15. Chief of Naval Research 1
800 N. Quincy Street
Arlington, VA 22217

16. Office of Naval Research (Code 480) 1
Naval Ocean Research and Development
Activity
NSTL Station
Bay ST. Louis, MS 39522

17. Commander 1
Oceanographic Systems Pacific
Box 1390
Pear Harbor, HI 96860

18. Officer in Charge 1
Naval Oceanography Command Detachment
Monterey, CA 93940

200456

Thesis
G713 Graves
c.1 Tactical application of an atmospheric mixed-layer model.

20 FEB 84
5 DEC 88

29066
80031

200456

Thesis
G713 Graves
c.1 Tactical application of an atmospheric mixed-layer model.

Tactical application of an atmospheric in

3 2768 002 13850 5
DUDLEY KNOX LIBRARY